Is Aromaticity Essential for Trapping the Catalytic Histidine 447 in Human Acetylcholinesterase?†

Dana Kaplan,‡ Dov Barak,§ Arie Ordentlich,‡ Chanoch Kronman,‡ Baruch Velan,‡ and Avigdor Shafferman*,‡

Departments of Biochemistry and Molecular Biology and of Organic Chemistry, Israel Institute for Biological Research, Ness-Ziona 74100, Israel

Received September 16, 2003; Revised Manuscript Received December 29, 2003

ABSTRACT: Replacement of both the acyl pocket residue Phe295 as well as residue Phe338, adjacent to the catalytic His447 in human acetylcholinesterase (HuAChE), resulted in a 680-fold decline in catalytic activity due to conformational destabilization of the histidine side chain [Barak et al. (2002) *Biochemistry 41,* 8245]. A possible restriction of this catalytically nonproductive mobility of His447 in a series of F295X/F338A HuAChEs was examined in silico followed by site-directed mutagenesis. Simulations suggested that of the 12 aliphatic residues substituted at position 295, including hydrophobic and polar amino acids, only methionine was capable of maintaining the catalytically viable conformation of His447. Examination of the reactivities of the actual F295X/F338A HuAChEs showed that indeed the F295M/F338A enzyme was only 2-fold less reactive than the F338A mutant toward acetylthiocholine, while enzymes substituted by the similarly bulky residues leucine and isoleucine were catalytically impaired. Furthermore, only the F295M/F338A enzyme exhibited wild-type-like reactivity toward covalent modifiers of the catalytic Ser203 including the methylphosphonate soman and transition state analogue *m*-(*N*,*N*,*N*-trimethylammonio)trifluoroacetophenone (TMTFA), as well as a facile dealkylation of the F295M/F338A−soman adduct. A different behavior was observed for bulkier ligands which introduce a deformation in the acyl pocket, and therefore their activity seems only marginally affected by the positioning of His447. The findings emphasize the importance of the precise positioning of His447 for catalysis and indicate that, in the absence of aromatic "trapping", restriction of the histidine mobility in F295X/F338A HuAChEs requires a combination of steric interference and a specific polar interaction. The results also underscore the role of the acyl pocket subsite of cholinesterases in maintaining the catalytically viable conformation of the catalytic histidine.

The precise juxtaposition of the catalytic histidine, relative to other elements of the catalytic triad, is thought to be imperative for optimal hydrolytic activity of cholinesterases[1] (ChEs) (*1*−*3*). In human acetylcholinesterase (HuAChE) such positioning of the catalytic His447(440)[2] is achieved through an array of interactions with acidic and aromatic residues adjacent to the active center (*4*−*6*). Recently, specific replacement by alanine of residues Phe295(288) and Phe338(331), vicinal to the imidazole moiety of His447, was shown to result in a pronounced decrease of hydrolytic activity of the mutated enzyme (*7*). Molecular simulations of this catalytically impaired F295A/F338A HuAChE indicated that the His447 side chain tends to assume a different average conformation from that observed in the X-ray structure of HuAChE (*7*, *8*). Such relationship between the HuAChE catalytic activity and conformational mobility of His447 is consistent with our conclusions from previous studies on the effects of perturbing the aromatic lining of the HuAChE active center gorge (*5*, *9*, *10*).

The significance of the aromatic stabilization of His447 was further demonstrated by engineering of a compensating interaction into the F295A/F338A HuAChE, through introduction of an aromatic residue in position 407(400) (*7*). Molecular dynamics simulations indicated that the wild-type-like conformation of residue His447 should be restored in the F295A/F338A/V407F HuAChE, and the engineered enzyme indeed exhibited a nearly 200-fold increase in catalytic activity relative to the F295A/F338A mutant (*7*). In the triple HuAChE mutant, as in the F295A and F338A HuAChEs, there is at least one potential His447−aromatic interaction, while in the catalytically impaired F295A/F338A HuAChE there seems to be none.

While the polar interactions of His447 with Glu334(327) and Glu202(199) are important in orienting the imidazole

† This work was supported by the U.S. Army Research and Development Command, Contracts DAMD17-00-C-0021 and DAMD17-03-C-0012 (to A.S.).

* Corresponding author. Tel: (972) 8-9381595. Fax: (972) 8-9401404. E-mail: avigdor@iibr.gov.il.

‡ Department of Biochemistry and Molecular Biology, Israel Institute for Biological Research.

§ Department of Organic Chemistry, Israel Institute for Biological Research.

[1] Abbreviations: ACh, acetylcholine; AChE, acetylcholinesterase; ATC, acetylthiocholine; BChE, butyrylcholinesterase; BTC, butyrylthiocholine; ChE, cholinesterase; DFP, diisopropyl phosphorofluoridate; HI-6, 1-(2-hydroxyiminomethylpyridinium)-1-(4-carboxyaminopyridinium) dimethyl ether dichloride; HuAChE, human acetylcholinesterase; soman, 1,2,2-trimethylpropyl methylphosphonofluoridate; TcAChE, *Torpedo californica* acetylcholinesterase; TMTFA, *m*-(*N*,*N*,*N*-trimethylammonio)trifluoroacetophenone.

[2] Amino acids and numbers refer to HuAChE, and the numbers in parentheses refer to the positions of analogous residues in TcAChE according to the recommended nomenclature (*32*).

10.1021/bi030206n CCC: $27.50
Published on Web 02/26/2004

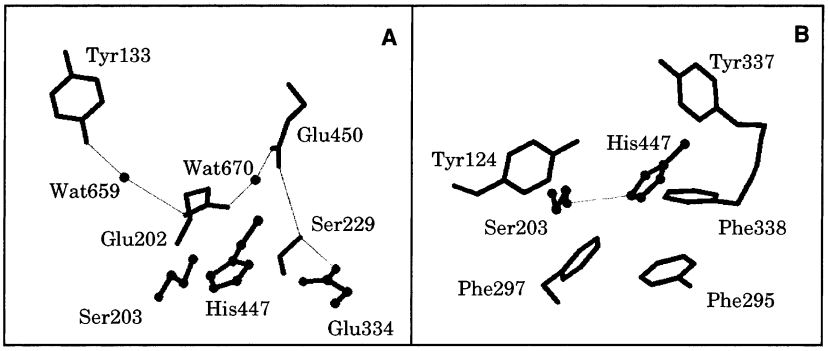

FIGURE 1: Molecular environment of the catalytic histidine in HuAChE. The catalytic triad comprised of Ser203, Glu334, and His447 is shown as balls and sticks. H-bond interactions are depicted as thin lines. (A) The immediate electrostatic environment of His447 is provided by Glu334 and Glu202, which in turn are stabilized and interconnected by H-bond interactions involving residues Tyr133, Ser229, and Glu450 and water molecules (Wat659 and Wat670) and constitute the H-bond network (*9*, *12*). (B) Aromatic interactions with His447 are observed mainly with residues Phe338 and Phe295, located within 4.47 and 5.70 Å, respectively (distances between centroids of the respective aromatic moieties). The proper orientation of these residues seems to be maintained through the Phe338−Phe295 interaction as well interactions of these residues with Tyr337, Phe297, and Tyr124.

moiety as well as in influencing its reactivity characteristics (*6*, *9*, *10*), the nature of the necessary His447−aromatic interaction is not clear (see Figure 1). It was already concluded that specific $\pi-\pi$ or cation$-\pi$ interactions between the side chains of residues His447 and Phe338 are required for facilitating the aging processes of certain phosphono-HuAChE conjugates (*6*, *9*, *11*). On the other hand, the catalytic activity of HuAChE is practically unaffected by removal of the aromatic residue from position 338 (*12*), indicating that the reactivity characteristics of His447 required for the two processes may be somewhat different. While specific interaction stabilizing the imidazolium moiety juxtaposed with the phosphonyl oxygen is required for the dealkylation of the phosphono-HuAChE (*6*, *7*, *9*), analogous stabilization of His447 appears to be unnecessary for catalysis of the hydrolytic reaction, provided it is properly oriented with respect to the catalytic Ser203(200). Thus, it may still be possible to achieve wild-type-like catalytic activity of HuAChE, which does not carry aromatic residues at positions 295 and 338, provided the amino acid at position 295 is bulky enough to restrict the mobility of His447 through van der Waals interactions.

In the present study we examine this hypothesis through generation of a series of doubly mutated forms of HuAChE, containing Ala338 and 12 different aliphatic substitutions at position 295. Our findings demonstrate that while His447−aromatic interaction is not imperative for maintaining the proper histidine conformation for efficient catalysis in HuAChE, the nonproductive mobility of His447 cannot be eliminated only by steric restriction due to bulky aliphatic residues at position 295. A combination of both steric interference and specific polar interactions is required, as demonstrated by different effects of the various bulky aliphatic amino acids at position 295 of the F295X/F338A HuAChE. The results also underscore the significance of the precise positioning of the His447 side chain to catalytic activity and the role of the acyl pocket subsite in maintaining the catalytically viable conformation of this histidine.

MATERIALS AND METHODS

Enzymes Reagents and Inhibitors. Mutagenesis of AChE was performed by DNA cassette replacement into a series of HuAChE sequence variants, which conserve the wild-type coding specificity (*13*) but carry new unique restriction sites (*14*−*16*).

The F338A mutant was constructed using the AChE-w8 neo-cat vector. Generation of the AChE-w8 neo-cat vector was accomplished by replacement of the *Mlu*I−*Sbf*I DNA fragment of the AChE-w7 cDNA variant (*17*) with the respective synthetic DNA duplexes carrying a new unique *Pac*I restriction site. The F338A mutation was carried out by replacement of the *Pac*I−*Nar*I DNA fragment of the AChE-w8 neo-cat vector with the respective synthetic DNA duplexes carrying the F338A mutation. In the synthetic *Pac*I−*Nar*I fragment the TTT codon of Phe338 was changed to GCC(Ala).

The double mutant F295A/F338A was generated by replacements of the *Mlu*I−*Pac*I DNA fragment of the F338A cDNA variant with the respective synthetic DNA duplexes carrying the mutated codon of F295A. In the synthetic *Mlu*I−*Pac*I fragment the TTC codon of Phe295 was changed to GCC(Ala). Construction of the double mutants related to the F295X/F338A series, carrying a specific substitution at position 295, was carried out at the same way, using the appropriate synthetic DNA duplex fragments. The synthetic *Mlu*I−*Pac*I fragments were all identical, except for the change at the codon sequence, coding to amino acid at position 295.

For the F295L/F338A, F295R/F338A, F295W/F338A, F295I/F338A, F295S/F338A, and F295Q/F338A variants we used the CTG(Leu), CGG(Arg), TGG(Trp), ATC(Ile), TCC-(Ser), and CAG(Gln) codons, respectively. F295N/F338A and F295T/F338A mutants were generated together, using degenerated synthetic fragments, carrying the degenerative codon sequences A(A/C)C. Also, for the F295K/F338A, F295M/F338A, F295E/F338A, and F295V/F338A mutants we used degenerative (A/G)(A/T)G codons for the formation of AAG(Lys), ATG(Met), GAG(Glu), and GTG(Val). F295Y/F338A and F295D/F338A mutants were constructed using the synthetic fragment with degenerative (T/G)AC codons, TAC(Tyr) and GAC(Asp).

Generation of F295A and F295L mutants was described previously (*17*). F295Y, F295D, F295R, and F295M mutants were constructed by replacing the *Mlu*I−*Pac*I DNA fragment of the AChE-w8 neo-cat vector with the appropriate synthetic DNA duplexes carrying the respective codon at position 295.

All of the synthetic DNA oligodeoxynucleotides were prepared using the automatic Applied Biosystems DNA synthesizer. The sequences of all clones were verified by the ABI PRISM BigDye terminator reaction kit, using the ABI310 genetic analyzer (Applied Biosystems).

Procedures of transfection of the human embryonal kidney-derived cell line (HEK-293) with expression vectors of recombinant enzymes and the generation of stable cell clones expressing high levels of each of the various recombinant products were described previously (*14*−*16*).

Acetylthiocholine iodide (ATC), 5,5′-dithiobis(2-nitrobenzoic acid) (DTNB), and diisopropyl phosphorofluoridate (DFP) were purchased from Sigma. *m*-(*N*,*N*,*N*-trimethylammonio)trifluoroacetophenone (TMTFA) was prepared according to the procedure described by Nair et al. (*18*). Preparation of the racemic mixtures of 1,2,2-trimethylpropyl methylphosphonofluoridate (soman) followed an accepted procedure using methylphosphonodifluoride and the appropriate alcohol (*10*).

1-(2-Hydroxyiminomethylpyridinium)-1-(4-carboxyaminopyridinium) dimethyl ether dichloride (HI-6) was a gift from Dr. G. Amitai.

Determination of HuAChE Activity and Analysis of Kinetic Data. Activity of HuAChE enzymes was assayed according to Ellman et al. (*19*) (in the presence of 0.1 mg/mL BSA, 0.3 mM DTNB, 50 mM sodium phosphate buffer, pH 8.0, and various concentrations of ATC/BTC), carried out at 27 °C and monitored by a Thermomax microplate reader (Molecular Devices). The enzyme concentration was determined by ELISA (*16*) and by active site titration (*15*) using the purified P*s*C*s*-soman stereomer (*9*, *20*).

Michaelis−Menten constants (K_m) and the apparent first-order rate constants k_{cat} were determined according to the kinetic treatment described before (*2*, *16*). The apparent bimolecular rate constants k_{app} were calculated from the ratio k_{cat}/K_m.

The apparent first-order rate constants for the time-dependent inhibition of the wild-type HuAChE and its mutants by TMTFA were determined by periodical measurement of the initial rate of substrate hydrolysis of aliquots taken from the reaction mixture. Following the kinetic treatment described by Nair et al. (*18*, *21*) and assuming a two-state inhibition mechanism, the values of k_{on} and k_{off} could be estimated from the linear plots of k_{obs} vs inhibitor concentration according to the equation:

$$k_{obs} = k'_{on}[\text{TMTFA}] + k_{off} \quad (1)$$

Since in aqueous solution TMTFA is a mixture of the free ketone ($TMTFA_{ket}$) and the ketone hydrate ($TMTFA_{hyd}$), corrected values of the association rate constants were obtained from $k_{on} = k'_{on}(1 + [TMTFA_{hyd}]/[TMTFA_{ket}])$, using the ratio of hydrated and ketone forms of TMTFA (62500) as determined by ^{19}F NMR (*18*).

Measurements of phosphylation rates were carried out in at least four different concentrations of DFP or soman (*I*), and residual enzyme activity (*E*) at various time points was monitored. The apparent bimolecular phosphonylation rate constants (k_i) determined under pseudo-first-order conditions were computed from the slopes of the plots of ln *E* versus time at different inhibitor concentrations. Rate constants under second-order conditions were determined from plots of $\ln\{E/[I_0 - (E_0 - E)]\}$ versus time (*9*).

Measurements of the rates of aging for soman adducts of the F338A, F295A/F339A, F295L/F338A, and F295M/F338A HuAChEs were carried out after inhibition of 98% of the initial enzyme activity. The inhibited enzymes were obtained under conditions where the rate of phosphonylation is much faster than the rate of aging. Excess soman was rapidly removed by column filtration (Sephadex G-15). The nonaged−soman conjugate fraction was assessed by reactivation with 0.5 mM HI-6 (under conditions where the rate of reactivation is faster than the rate of aging; *22*). The first-order rate constants of aging (k_a) were determined from slopes of ln E_r versus time.

Molecular Dynamics Simulation. Simulations of the wild-type and the F295X/F338A HuAChEs were performed using the AMBER 5.0 suite of programs with the all-atom parameter set. Characterization and visual examination of the molecular structures were done using the molecular modeling package SYBYL 6.7 running on an SGI Octane workstation. The starting conformation of the wild-type enzyme was obtained from the X-ray structure of the HuAChE−fasciculin complex model (*8*; structure 1b41 in the Protein Data Bank). The essential water molecules Wat659 and Wat670 (*7*, *8*) were retained throughout the simulations. The rim of the active site gorge as well as the active center was solvated by adding a spherical cap of water (using the SOL option of AMBER). The cap waters were restrained by soft half-harmonic potential to avoid evaporation without affecting the protein movement. The part of the HuAChE molecule included in the simulation (using the belly option in AMBER) was comprised of residues in and around the active center gorge (about 150 residues were included; the number varied slightly depending upon the definition of the belly region for the specific simulation experiments). Models of the HuAChE mutants were obtained by optimization of the appropriately modified structures, initially with restrained backbone, followed by minimization of the totally relaxed structure. Initially, all of the structures were equilibrated at 300 K (20 ps), followed by 200 ps of dynamics runs of the wild-type HuAChE at both 300 and 400 K. No significant differences in the average structure of the active center could be observed due to the different simulation conditions. Consequently, all of the production runs were carried out at 400 K in order to avoid the excessively long simulation times.

RESULTS AND DISCUSSION

Enhanced conformational mobility of the catalytic histidine His447 in HuAChE was recently implicated in the 680-fold decrease in the catalytic activity of the double mutant F295A/F338A (*7*). This enzyme was specifically designed to introduce conformational mobility of the His447 side chain through removal of aromatic residues from its immediate vicinity. As already indicated (*7*), such ability to modify the conformational properties of His447, through manipulation of its aromatic environment, may result from perturbation of the "aromatic trapping". Yet, it is also possible that the enhanced mobility of His447 is simply a result of creating a void around the His447 side chain due to removal of bulky aromatic residues.

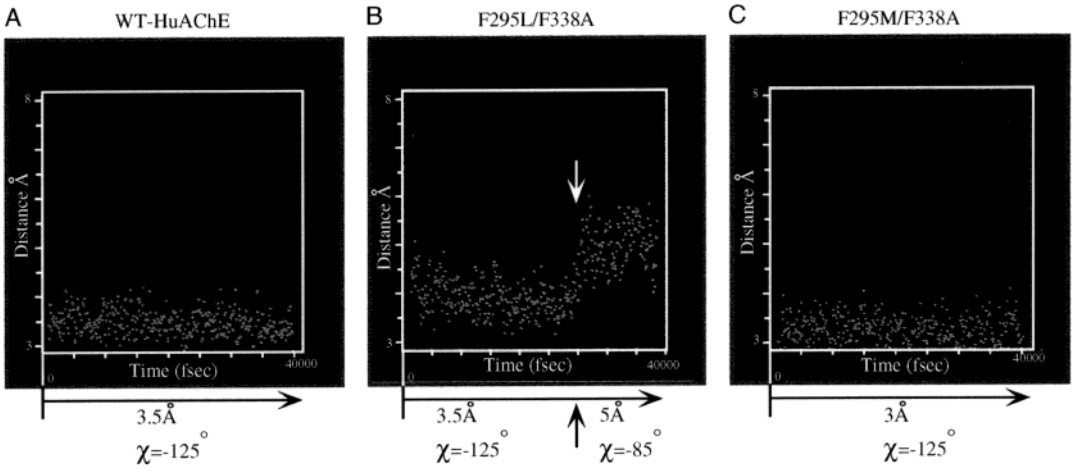

FIGURE 2: Examination of conformational mobility of the catalytic histidine side chain by molecular dynamics simulation. Depicted are 40 ps segments of the simulations performed on wild-type HuAChE and on representative cases of a series of double-mutated forms of F295X/F338A. (A) Wild-type HuAChE. The side chain of His447 maintains an average distance, between ϵ^2N−His447 and γO−Ser203, and a dihedral angle, between the imidazolium moiety of His447 and the backbone, of 3.5 Å and $\chi = -125°$ throughout the simulation. (B) F295L/F338A represents a model for the type I dynamic phenotype (Table 1) of His447. The side chain of His447 tends to assume a different average conformation during the simulation, changing the average ϵ^2N−γO distance and dihedral angle between the imidazolium moiety and the backbone to 5 Å and $\chi = -85°$, respectively. (C) F295M/F338A, in which His447 maintained a wild-type-like orientation throughout the simulation, with an average distance and dihedral angle of 3 Å and $\chi = -125°$, respectively.

The possibility that certain aliphatic replacements at position 295 may compensate for the perturbation in the positioning of His447, created by removing aromatic residues from positions 295 and 338, was tested through in silico mutagenesis of HuAChE and simulation of the effects of various replacements at position 295 on the mobility of residue His447. Molecular models of F295X/F338A HuAChEs, where X stands for various aliphatic residues, were built and the average conformations of the corresponding His447 side chain examined for each case by molecular dynamics. The starting structure used in these simulations was taken from the X-ray structure of the HuAChE−fasciculin complex (*8*) by removing the ligand and relaxing the regions of contact (*7*). The average dihedral angle between the imidazolium moiety of His447 and the backbone and the average distance ϵ^2N-His447−γO-Ser203 were −125° and 3.5 Å, respectively, throughout the simulations of wild-type HuAChE (*5*; see Figure 2A). Substitution of the phenylalanine residues at positions 295 and 338 by alanine resulted in an enzyme (F295A/F338A) for which, as already reported, the average dihedral angle was found to be −80° and the ϵ^2N−γO distance 5.0 Å (*7*). With respect to the position of His447 these values (corresponding to the structures of the wild-type and F295A/F338A HuAChEs) were expected to define the limits of the histidine side chain mobility since other residue substitutions at position 295 introduce bulkier moieties into its vicinity.

Molecular dynamics simulations of F295X/F338A HuAChE models, carrying small aliphatic residues (volumes of residue X were in the range 88.6−143.9 Å^3, corresponding to alanine−glutamine; for comparison, the volume of phenylalanine is 189 Å^3; see ref *23*, Table 1, and Figure 3), resulted consistently in an altered average conformation of His447. The range of conformations in the different models is quite narrow (with dihedral angles of the histidine side chains of −80 to −95° and ϵ^2N−γO distances of 5.0−7.0 Å), indicating that the His447 conformational properties are independent of residue X. For F295X/F338A HuAChE models bearing bulkier aliphatic residues (162−173.4 Å^3; see also Figure 3), the simulated conformational behavior of His447 seems to depend on the nature of the specific residue at position 295. Thus, while for the hydrophobic residues leucine and isoleucine altered average conformations of His447 were observed, in the F295M/F338A HuAChE model residue His447 maintained wild-type-like orientation with an average dihedral angle of −125° and ϵ^2N−γO distance of 3.0 Å (Figure 2B,C). For F295R/F338A the simulated average dihedral angle of His447 was −85° despite the fact that arginine is the bulkiest aliphatic residue and in this respect resembles most closely phenylalanine (*23*; see Table 1 and Figure 3). In this case, as in the case of lysine, repulsive electrostatic interactions with the His447−imidazolium moiety may contribute to its mobility.

These results seem to suggest that the optimal functional conformation of His447 in F295X/F338A HuAChE *cannot be maintained by aliphatic amino acids at position 295 with the notable exception of methionine*. The finding that a functional conformation of His447 is maintained in the F295M/F338A HuAChE model, although methionine is a little less bulky than leucine or isoleucine (Figure 3), implies an involvement of specific interaction with the imidazole moiety. Such interaction is probably similar to interactions of sulfur with other aromatic moieties, which are quite common for side chains of aromatic amino acids (*24*).

Examination of catalytic efficiency for the F295X/F338A HuAChEs revealed that indeed F295M/F338A HuAChE is only 6-fold less active than the wild-type enzyme and remarkably 100-fold more active than the F295A/F338A HuAChE. Furthermore, as predicted by molecular simulations, a pronounced decline of the hydrolytic activity (>110-fold) for all of the F295X/F338A enzymes carrying small aliphatic amino acids at position 295 has been observed (Table 1). The activities of enzymes carrying hydrophobic residues like alanine or valine are quite similar to those substituted by polar residues such as asparagine or glutamine, further supporting the notion that a common mechanism, like

Table 1: Effects of Various Replacements at Position 295 of F295X/F338A HuAChE on the Catalytic Activity[a] and Conformational Mobility[b] of His447

AChE type	volume of AA[c] at position 295 (Å^3)	dynamic phenotype of His447[b]	ATC hydrolysis[a] K_m (mM)	k_{cat} ($\times 10^{-5}$) (min^{-1})	k_{app} ($\times 10^{-8}$) (M^{-1} min^{-1})	rel k_{app} WT/mutant
Phe295/Phe338 (WT)	189.0	WT	0.15	5.1	34	1
Phe295/Phe338Ala	189.0	WT	0.24	2.4	10	3
Phe295Ala/Phe338Ala	88.6	type I	4.9	0.24	0.05	680
Phe295Ser/Phe338Ala	89.0	ND[d]	5.2	0.22	0.04	800
Phe295Asp/Phe338Ala	111.1	type I	5.7	0.08	0.014	2400
Phe295Thr/Phe338Ala	116.0	type I	14	0.16	0.01	3400
Phe295Asn/Phe338Ala	117.1	type I	1.0	0.3	0.3	110
Phe295Gln/Phe338Ala	138.4	type I	3.0	0.15	0.05	680
Phe295Val/Phe338Ala	140.0	type I	1.7	0.15	0.09	380
Phe295Glu/Phe338Ala	143.9	type I			<0.001	>30000
Phe295Met/Phe338Ala	162.0	WT	0.22	1.3	5.9	6
Phe295Ile/Phe338Ala	166.0	type I	5.0	0.16	0.03	1130
Phe295Leu/Phe338Ala	166.6	type I	0.3	0.2	0.67	55
Phe295Lys/Phe338Ala	168.0	type I			<0.001	>30000
Phe295Arg/Phe338Ala	173.4	type I	1.2	0.007	0.006	5700
Phe295Tyr/Phe338Ala	193.6	WT	0.8	0.2	0.25	140
Phe295Trp/Phe338Ala	227.8	type I	0.3	0.2	0.67	55

[a] Values represent the mean of triplicate determinations with the standard deviation not exceeding 20%. [b] Simulated prototypical average conformations of His447 described in terms of the Cα−Cβ dihedral angle (χ) and the $^{\epsilon 2}$N-His447−$^{\gamma}$O-Ser203 distance (d). WT: $\chi = -125°$, $d =$ 3.5 Å. Type I: $\chi = -100$ to $-85°$, $d = 4-7$ Å. [c] According to ref *23*. [d] Not done.

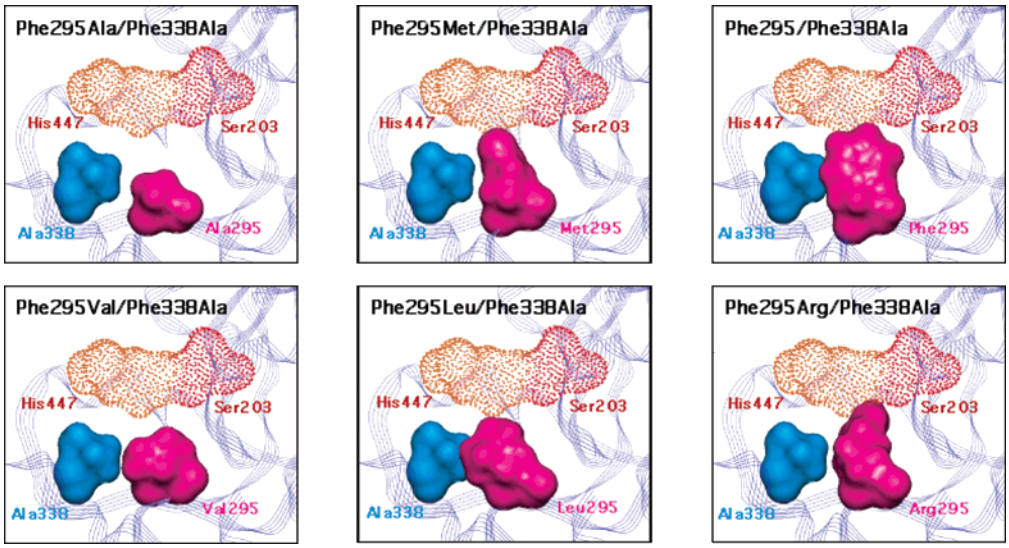

FIGURE 3: Putative orientation of selected aliphatic amino acids at position 295 of the F295X/F338A HuAChE with respect to the catalytic His447. Note that when position 295 is occupied with alanine or valine, no interaction with His447 can be observed. For methionine, leucine, and arginine at position 295 the respective molecular volumes are similar and allow for interaction with His447, in an analogous manner to that shown for Phe295/Phe338Ala. Yet only for Phe295Met/Phe338Ala as in Phe295/Phe338Ala do molecular simulations indicate that this interaction is sufficient to prevent mobility of His447.

displacement of the His447 imidazole moiety, is the underlying cause for their catalytic deficiency. The F295X/F338A HuAChEs substituted at position 295 by acidic or hydroxylic polar residues (Asp, Glu, or Thr) are even more catalytically compromised (see Table 1), suggesting that in addition to the effect on mobility of His447 these residues may introduce a direct electrostatic perturbation of the active site environment, due to the proximity of position 295 substituents to the catalytic Ser203. Such a notion is consistent with the low catalytic activity observed for the corresponding single mutant at position 295 (F295D HuAChE; see Table 2) which can be associated more directly with the polarity of the side chain.

In the cases of the large basic residues arginine and lysine, electrostatic interactions with His447 may again contribute to the pronounced decrease in catalytic activities of the corresponding F295X/F338A HuAChEs relative to the F338A enzyme (Table 1). Similar interactions in the F295R HuAChE can probably account for the low catalytic activity of this enzyme (Table 2). Thus, although the side chains of arginine and lysine seem to fill the void next to His447 in the corresponding F295X/F338A HuAChEs (see Figure 3), the histidine side chain still tends to assume the nonreactive conformation. For the F295X/F338A enzymes carrying aromatic residues at position 295, molecular dynamics simulations indicate that positioning of His447 in the F295Y/F338A HuAChE resembles that in the F338A enzyme. Such an outcome seems consistent with the similar volumes of phenylalanine and tyrosine, yet catalytic activity of the F295Y/F338A HuAChE was found to be nearly 50-fold

Table 2: Kinetic Parameters[a] of Hydrolysis of Acetylthiocholine by HuAChE and Its Mutants

AChE type	K_m (mM)	k_{cat} ($\times 10^{-5}$) (min^{-1})	k_{app} ($\times 10^{-8}$) (M^{-1} min^{-1})	rel k_{app} WT/mutamt
WT	0.15	5.1	34.0	1
Phe295Ala	0.13	3.8	29.0	1.2
Phe295Met	0.13	2.5	19.2	1.8
Phe295Tyr	0.05	0.4	8.0	4
Phe295Leu	0.20	1.2	6.0	6
Phe295Asp	4.10	0.6	0.14	240
Phe295Arg	3.40	0.04	0.01	3400

[a] Values represent the mean of triplicate determinations with the standard deviation not exceeding 20%.

lower than that of the F338A enzyme. The reason for this apparent discrepancy may be found in the proximity of the $^{\eta}$O-Y295 to the catalytic Ser203. In fact, the value of k_{cat} for the F295Y HuAChE is nearly as low as that of the F295Y/F338A enzyme (Tables 1 and 2), suggesting that in this case the decline in catalytic activity has nothing to do with the conformational properties of His447. In the case of F295W/F338A HuAChE, the aromatic moiety of tryptophan is apparently too bulky to be accommodated in the available space next to His447, and consequently the side chain of the latter is displaced due to steric congestion or due to distortion of the acyl pocket. In this context it should be mentioned that since all of the molecular simulation experiments were carried out in the absence of ligands, the results may be indicative only in cases where formation of the enzyme−ligand conjugate does not produce deformation of the acyl pocket. If such deformation takes place, due to steric pressure of the ligand or a large residue such as tryptophan at position 295, the molecular environment of His447 may no longer resemble the one used for our simulations.

The F295X/F338A HuAChEs bearing the three large hydrophobic amino acids, leucine, isoleucine, and methionine, constitute the most interesting cases in the present study since the bulk of these residues at position 295 seems large enough to provide a steric barrier to His447 movement (Figure 3). Yet the F295I/F338A and F295L/F338A HuAChEs exhibit low catalytic activity compared to the F338A enzyme (Table 1). These results are consistent with the prediction based on their simulated mobility of His447 and underscore the unique catalytic behavior of the corresponding double mutant bearing methionine at position 295. For the latter, the values of both K_m and k_{cat} are very similar to those of the F338A HuAChE, indicating that His447 is properly positioned both for participating in the accommodation of the planar substrate and for its functions in the catalytic reactions. The wild-type-like value of K_m for the F295M/F338A HuAChE signifies also that the overall architecture of the active center, probed by the noncovalent interactions with ATC, is similar to that of the wild-type enzyme. A relatively low value of K_m is observed also for the F295L/F338A HuAChE, yet the low value of the corresponding k_{cat} suggests that His447 is not optimally oriented for catalysis. On the other hand, the F295I/F338A HuAChE, which exhibits a similarly low value of k_{cat}, shows also a high value of K_m (equivalent to that of the F295A/F338A enzyme). Thus it appears that the difference between leucine and isoleucine at position 295 of the F295X/F338A HuAChE is in a direct interaction of these residues with ATC in the respective Michaelis complexes, rather than in different conformational properties of His447.

To further examine the different effect of substituting methionine and the other hydrophobic residues leucine and isoleucine at position 295, we compared the reactivities of the F295L/F338A, F295I/F338A, and F295M/F338A enzymes toward the active center irreversible phosphonate inhibitor soman and the transition state analogue TMTFA. It is believed that in AChEs rapid initial formation of the noncovalent Michaelis complex with the tetrahedral phosphonate inhibitor precedes the much slower covalent reaction with the enzyme (*9*, *26*−*28*). Reactions with TMTFA involve rapid formation of covalent tetrahedral intermediates, probing mainly the characteristics of His447 during the catalytic reactions. Thus, in both cases His447 is involved in stabilization of tetrahedral species in the active center, a function which seems always impaired by its enhanced mobility.

The results show unequivocally that reactivities of the F295L/F338A and F295I/F338A HuAChEs toward soman and TMTFA differ from that of the corresponding enzyme substituted by methionine at position 295 (Table 3). Furthermore, the rate constants of phosphonylation as well as those of adduct formation with TMTFA resemble those for the F295A/F338A HuAChE, indicating that, with respect to interaction with tetrahedral species, the bulky residues at position 295 do not contribute to the stabilization of His447 any more than alanine. On the other hand, reactivity of the F295M/F338A enzyme toward both soman and TMTFA closely resembled that of the wild-type HuAChE (see Table 3). Such a clear-cut distinction between reactivity phenotypes of the F295X/F338A enzymes resembling F295A/F338A (F295L/F338A; F295I/F338A) and wild-type (F295M/F338A) HuAChEs is also consistent with the prediction from simulation experiments regarding the two rather discrete conformational states of the His447 side chain. Thus, for ligands that do not introduce steric perturbation in the acyl pocket, reactivity can be correlated quite well with the conformational properties of His447.

The relatively low reactivity of HuAChE toward the substrate BTC and the phosphate DFP (Table 3) has been thought to result from steric congestion of the substituent accommodated in the acyl pocket. This notion was recently supported by the X-ray structure of the DFP−TcAChE conjugate where the phosphoryl isopropoxy group distorted the acyl pocket, changing the mutual orientation of residues in the immediate vicinity of the catalytic histidine. Therefore, the pattern of changes in reactivity toward BTC and DFP, following variations of substitution at position 295 of the F295X/F338A enzymes, should differ from that observed in the cases of ATC, soman, and TMTFA. In fact, the most reactive HuAChE enzymes toward DFP were F295L/F338A and F295M/F338A, with phosphylation constants respectively 50-fold and 13-fold higher than that of the F338A HuAChE (Table 3). The corresponding reactivity of the F295I/F338A enzyme is similar to that of the wild-type enzyme and only 4-fold higher than that of F338A HuAChE. Similar reactivity patterns could be observed toward BTC, further suggesting that for these cases "trapping" of His447 may not be a major determinant of the reactivity of F295X/F338A HuAChEs.

The kinetic properties of the F295X/F338A enzymes examined in this study demonstrate that although the

Table 3: Kinetic Constants[a] of Various F295X/F338A HuAChEs Carrying Different Hydrophobic Substitutions at Position 295

AChE type	ATC k_{app} ($\times 10^{-8}$) (M^{-1} min^{-1})	TMTFA k_{on} ($\times 10^{-4}$) (M^{-1} min^{-1})	soman k_i ($\times 10^{-4}$) (M^{-1} min^{-1})	BTC k_{app} ($\times 10^{-8}$) (M^{-1} min^{-1})	DFP k_i ($\times 10^{-4}$) (M^{-1} min^{-1})
Phe295/Phe338 (WT)	34	190	10000	0.3	10
Phe295/Phe338Ala	10	400	10000	0.05	2
Phe295Ala/Phe338Ala	0.05	20	100	0.9	4
Phe295Ile/Phe338Ala	0.03	8	140	0.24	8
Phe295Leu/Phe338Ala	0.67	35	130	1.5	100
Phe295Met/Phe338Ala	5.9	250	8000	2.2	25

[a] Values represent the mean of triplicate determinations with the standard deviation not exceeding 20%.

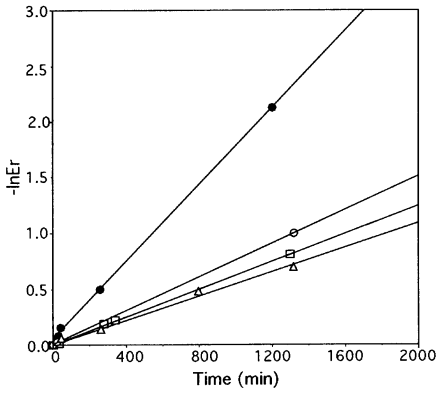

FIGURE 4: Comparison of the rates of aging for soman adducts of the different F338A HuAChE mutants: F338A (□), F295A/F338A (Δ), F295L/F338A (○), and F295M/F338A (●) HuAChEs.

aromatic nature of the residue at position 295 is not a prerequisite for maintaining a nearly wild-type-like HuAChE catalytic activity, effective trapping of the catalytic histidine cannot be achieved solely by bulky aliphatic amino acids, such as leucine or isoleucine. According to molecular models these two residues, as well as methionine, appear to fill the void next to the His447 imidazolium moiety, and therefore steric effect cannot be the dominant factor in orienting the side chain of His447 in the F295M/F338A HuAChE (Figure 3). Thus, a specific sulfur−imidazolium interaction, proposed already on the basis of molecular dynamics simulations, may contribute to the overall Met295−His447 interaction. Such a specific interaction with the imidazolium moiety is also consistent with the finding that the rate of dealkylation (aging) of the somanyl adduct of the F295M/F338A enzyme is 7-fold higher than that of the corresponding adduct of the F338A HuAChE, while the corresponding adduct of F295L/F338A ages at a rate similar to the adducts of F338A and F295A/F338A (Figure 4). Facility of such dealkylation processes of phosphonyl−HuAChE adducts was already shown to depend critically upon specific interactions stabilizing the imidazolium moiety (*6*, *9*, *11*). Analogous stabilization of His447 appears to be unnecessary for efficient catalysis of the hydrolytic reaction, provided its imidazole moiety is properly oriented with respect to the catalytic Ser203. Therefore, the enhanced aging of the somanyl−F295M/F338A adduct, relative to that of the corresponding F338A conjugate, suggests that in the F295M/F338A HuAChE trapping of His447 may be achieved through a combination of steric and electronic effects. Such an electronic effect could be similar to the sulfur−arene interactions, which is frequently observed for the side chains of methionine and aromatic amino acids (*22*) but, to the best of our knowledge, has not yet been invoked with respect to the aromatic moiety of histidine.

The conclusion that the catalytic histidine in HuAChE is partially trapped by the residue at position 295, which is also a part of the acyl pocket subsite, has interesting implications with respect to the mechanism of the enzyme substrate selectivity as well as its stereoselectivity toward chiral covalent modifiers such as methyl phosphonofluoridates (*9*, *17*). In the past it was generally assumed that AChE stereoselectivity toward covalent inhibitors such as sarin or soman was a result of exclusion of the respective alkoxy substituents from the acyl pocket (*9*, *25*). In this molecular scenario the acyl pocket was regarded as a relatively rigid structure with limited flexibility to accommodate steric pressures presented by the ligands. However, recent crystallographic studies of TcAChE conjugates demonstrate plasticity of the loop including the acyl pocket residues Phe288 and Phe290 (corresponding to Phe295 and Phe297 in HuAChE). In particular, large displacement of the acyl pocket polypeptide backbone atoms (nearly 5 Å) was observed in the TcAChE-DFP adduct (*29*), indicating that accommodation of a bulky ligand in the HuAChE active center involves a significant relocation of the side chains of both Phe295 and Phe297. This in turn may perturb the positioning of His447 and affect its ability to participate in accommodation of the ligand, very much as if the acyl pocket residues were replaced by aliphatic amino acids. Thus, perturbation of the His447 interaction with tetrahedral species may be the actual reason for the low reactivity of HuAChE toward P_R-diastereomers of methylphosphonates and, consequently, for its high stereoselectivity toward this class of inhibitors, rather than steric congestion. Such a view of the role of the residue at position 295 is also compatible with the variations of the acyl pocket structure observed in the different members of the ChE family. In invertebrate AChEs (from *Drosophila* or *Anopheles*) residues Leu328 (Phe295 in HuAChE) and Phe440 (Val407 in HuAChE) seem to participate in formation of the acyl pocket subsite (*30*). Such an altered acyl pocket does not provide substrate selectivity, since *Drosophila* AChE hydrolyzes BCh at about half the rate of ACh hydrolysis (*31*); however, it may function in an analogous manner to Phe295 (in HuAChE) with respect to positioning of the catalytic histidine. These speculations are in agreement with our previous work, showing that redesign of the environment of F295A/F338A-HuAChE by introducing of phenylalanine in position 407 restores most of the enzyme reactivity.

In conclusion, the conformational properties of the catalytic His447 in HuAChE, and thereby the catalytic properties of the enzyme, seem to be determined in part by $\pi-\pi$ interactions with residue Phe338 and by steric restriction due to residue Phe295. In F295M/F338A HuAChE the methionine at position 295 is capable of participating in both polar and

steric interactions and therefore in mimicking the aromatic trapping of His447. Furthermore, although participation of the acyl pocket in trapping of the catalytic histidine does not have to involve aromatic interactions, such a role of this active center subsite in ChEs seems even more significant to the optimal enzymatic activity than its presumed role in substrate selectivity.

ACKNOWLEDGMENT

We thank Dana Stein and Nehama Seliger for excellent technical assistance and contribution.

REFERENCES

1. Gibney, G., Camp, S., Dionne, M., MacPhee-Quigley, K., and Taylor, P. (1990) *Proc. Natl. Acad. Sci. U.S.A. 87*, 7546−7550.
2. Shafferman, A., Velan, B., Ordentlich, A., Kronman, C., Grosfeld, H., Leitner, M., Flashner, Y., Cohen, S., Barak, D., and Ariel, N. (1992) *EMBO J. 11*, 3561−3568.
3. Fuxreiter, M., and Warshel, A. (1998) *J. Am. Chem. Soc. 120*, 183−194.
4. Millard, C. B., Koellner, G., Ordentlich, A., Shafferman, A., Silman, I., and Sussman, J. L. (1999) *J. Am. Chem. Soc. 121*, 9883−9884.
5. Kaplan, D., Ordentlich, A., Barak, D., Ariel, N., Kronman, C., Velan, B., and Shafferman, A. (2001) *Biochemistry 40*, 7433−7445.
6. Shafferman, A., Ordentlich, A., Barak, D., Stein, D., Ariel, N., and Velan, B. (1996) *Biochem. J. 318*, 833−840.
7. Barak, D., Kaplan, D., Ordentlich, A., Ariel, N., Velan, B., and Shafferman, A. (2002) *Biochemistry 41*, 8245−8252.
8. Kryger, G., Harel, M., Giles, K., Toker, L., Velan, B., Lazar, A., Kronman, C., Barak, D., Ariel, N., Shafferman, A., Silman, I., and Sussman, J. L. (2000) *Acta Crystallogr. D56*, 1385−1394.
9. Ordentlich, A., Barak, D., Kronman, C., Benschop, H. P., De Jong, L. P. A., Ariel, N., Barak, R., Segall, Y., Velan, B., and Shafferman, A. (1999) *Biochemistry 38*, 3055−3066.
10. Barak, D., Ordentlich, A., Segall, Y., Velan, B., Benschop, H. P., De Jong, L. P. A., and Shafferman, A. (1997) *J. Am. Chem. Soc. 119*, 3157−3158.
11. Saxena, A., Doctor, B. P., Maxwelll, D. M., Lenz, D. E., Radic, Z., and Taylor, P. (1993) *Biochem. Biophys. Res. Commun. 197*, 343−349.
12. Ordentlich, A., Kronman, C., Barak, D., Stein, D., Ariel, N., Marcus, D., Velan, B., and Shafferman, A. (1993) *FEBS Lett. 334*, 215−220.
13. Soreq, H., Ben-Aziz, R., Prody, C. A., Seidman, S., Gnatt, A., Neville, L., Lieman-Hurwitz, J., Lev-Lehman, E., Ginzberg, D., Lipidot-Lifson, Y., and Zakut, H. (1990) *Proc. Natl. Acad. Sci. U.S.A. 87*, 9688−9692.
14. Velan, B., Grosfeld, H., Kronman, C., Leitner, M., Gozes, Y., Lazar, A., Flashner, Y., Marcus, D., Cohen, S., and Shafferman, A. (1991) *J. Biol. Chem. 266*, 23977−23984.
15. Kronman, C., Velan, B., Gozes, Y., Leitner, M., Flashner, Y., Lazar, A., Marcus, D., Sery, T., Papier, Y., Grosfeld, H., Cohen, S., and Shafferman, A. (1992) *Gene 121*, 295−304.
16. Shafferman, A., Kronman, C., Flashner, Y., Leitner, S., Grosfeld, H., Ordentlich, A., Gozes, Y., Cohen, S., Ariel, N., Barak, D., Harel, M., Silman, I., Sussman, J. L., and Velan, B. (1992) *J. Biol. Chem. 267*, 17640−17648.
17. Ordentlich, A., Barak, D., Kronman, C., Flashner, Y., Leitner, M., Segall, Y., Ariel, N., Cohen, S., Velan, B., and Shafferman, A. (1993) *J. Biol. Chem. 268*, 17083−17095.
18. Nair, H. K., Lee, K., and Quinn, D. M. (1993) *J. Am. Chem. Soc. 115*, 9939−9941.
19. Ellman, G. L., Courtney, K. D., Andres, V., and Featherstone, R. M. (1961) *Biochem. Pharmacol. 7*, 88−95.
20. Benschop, H. P., Konings, C. A. G., Van Genderen, J., and De Jong, L. P. A. (1984) *Toxicol. Appl. Pharmacol. 72*, 61−74.
21. Nair, H. K., Seravalli, J., Arbuckle, T., and Quinn, D. M. (1994) *Biochemistry 33*, 8566−8576.
22. Grosfeld, H., Barak, D., Ordentlich, A., Velan, B., and Shafferman, A. (1996) *Mol. Pharmacol. 50*, 639−649.
23. Singh, J., and Thornton, J. M. (1992) *Atlas of Protein Side-Chain Interactions*, Vol. 1, p 6, Oxford University Press, Oxford, U.K.
24. Meyer, E. A., Castellano, R. K., and Diederich, F. (2003) *Angew. Chem., Int. Ed. 42*, 1210−1250.
25. Barak, D., Ariel, N., Velan, B., and Shafferman, A. (1992) in *Multidisciplinary Approaches to ChE Functions* (Shafferman, A., and Velan, B., Eds.) pp 177−183, Plenum Press, New York.
26. Aldridge, W. N., and Reiner, E. (1972) *Enzyme Inhibitors as Substrates*, North-Holland Publishing Co., Amsterdam, The Netherlands.
27. Main, A. R. (1976) in *Biology of Cholinergic Function* (Goldberg, A. M., and Hanin, I., Eds.) pp 269−353, Raven Press, New York.
28. Ordentlich, A., Barak, D., Kronman, C., Ariel, N., Segall, Y., Velan, B., and Shafferman, A. (1996) *J. Biol. Chem. 271*, 11953−11962.
29. Millard, C. B., Kryger, G., Ordentlich, A., Greenblatt, H., Harel, M., Raves, M., Segall, Y., Barak, D., Shafferman, A., Silman, I., and Sussman, J. L. (1999) *Biochemistry 38*, 7032−7039.
30. Harel, M., Kryger, G., Rosenberry, T. L., Mallender, W. D., Lewis, T., Fletcher, R. J., Guss, J. M., Silman, I., and Sussman, J. L. (2000) *Protein Sci.*, 1063−1072.
31. Gnagey, A. L., Forte, M., and Rosenberry, T. L. (1987) *J. Biol. Chem. 262*, 13290−13298.
32. Massoulie, J., Sussman, J. L., Doctor, B. P., Soreq, H., Velan, B., Cygler, M., Rotundo, R., Shafferman, A., Silman, I., and Taylor, P. (1992) in *Multidisciplinary Approaches to Cholinesterase Functions* (Shafferman, A., and Velan, B., Eds.) pp 285−288, Plenum Press, New York.

BI030206N